Article

The numerical analysis of the heat transfer process in selected surfaces of the water boiler

Abdullah El Sabea [1*], Jacek Baranski [1], Paweł Dąbrowski [1]

[1] Faculty of Mechanical Engineering and Ship Technology, Gdańsk University of Technology, ul. Narutowicza 11/12, Gdańsk 80-233, Poland,
* Corresponding author: abdullah.sabea@hotmail.com

Abstract

The paper presents an analysis of the heat transfer process on heating surfaces made with different materials in a fire tube water boiler supplied by natural gas. The analysis was based on analytical calculations and numerical simulations using ANSYS Fluent software. The analytical calculations were performed to investigate the flue gas composition as a product of the natural gas combustion process and to apply these results in numerical modeling of heat transfer phenomena between hot exhaust gas and water in the boiler's heat exchanger. The obtained results show that optimization of heat exchanger design is crucial for efficient heat transfer process in every boiler, which has important implications for the energy efficiency of those systems and environmental protection due to fuel consumption reduction. This research provides valuable insights into the importance of heat exchanger design and its impact on the efficiency of water boilers.

Keywords: Thermodynamics, Water boiler, Heat exchanger, Heat transfer, Combustion process, Flue gas, CFD

Nomenclature

A	–	heat transfer area, m2
A_w	–	boiler wall area, m2
C_0	–	Stefan Boltzmann constant, W/(m²·K)
Cp	–	specific heat, J/(kg K)
D	–	hydraulic diameter, m
$\dot{E}_{ch}$	–	fuel chemical power supplied, W
G	–	mass flux, kg/(m²·s)
g	–	gravitational acceleration vector, -
h	–	specific enthalpy, J/kg
k	–	thermal conductivity, W/(m·K)
L	–	length, m
$\dot{m}_w$	–	mass flow rate, kg/s
P	–	pressure, Pa
P_{amb}	–	ambient pressure, Pa
P_{fuel}	–	fuel pressure and overpressure, Pa
$\dot{Q}_{uh}$	–	useful heat transfer rate, W
q	–	heat flux, W/m²
Q_i	–	calorific value of fuel, J/Nm^3
R	–	radius, m
T	–	temperature, °C
t	–	time, s
t_{fuel}	–	fuel temperature, °C
$T_{wall}{}'$	–	boiler wall temperature, K
T_{amb}	–	air ambient temperature, K
$\dot{V}_w$	–	volumetric flow rate, m³/s
$\dot{V}_{fuel}$	–	fuel volumetric flow rate, Nm^3/s
$V_{fluegas}$	–	amount of flue gas, $Nm^3/Nm^3 fuel$
V	–	Velocity, m/s

Greek symbols

α	–	convective heat transfer coefficient, W/(m²·K)
ρ	–	density, kg/m³
η_b	–	boiler efficiency, %
ε	–	boiler walls' emissivity, –
◎	–	air relative humidity, %
◎amb	–	air ambient relative humidity, %
τ	–	stress tensor, N/m²
ω	–	percentage deviation, %

1. Introduction

Hot water is an essential part of daily life, and water boilers play a critical role in ensuring its availability. According to the Water Heaters Global Market Report for 2022, the industry has experienced remarkable growth, with a compound annual growth rate of 16.5% from 2021 to 2022, and a projected market size of $53.58 billion by 2026 [1]. The efficiency of water boilers, particularly through heat exchanger optimization, is vital in this context.

Efficiency is a top priority in various mechanical and energy-related fields. The type of water boiler, operational mode, fuel type, and heat exchanger design significantly impact performance. Previous research has focused on enhancing heat transfer in heat exchangers using a variety of methods. For example, Rehman [2] investigated heat transfer coefficient optimization in a shell-and-tube heat exchanger using CFD simulations. Meanwhile, Rajeshkumar et al. [3] conducted a study on heat transfer analysis in fin and tube heat exchangers, demonstrating the potential for enhanced heat transmission through design modifications. Kaushik et al. [4] explored convective heat transfer in corrugated channels, revealing significant improvements with specific corrugation shapes.

Despite these advancements, there remains a need for novel and efficient heat exchanger designs that can further enhance heat transfer performance. Our current research focuses on developing a novel heat exchanger design that incorporates geometrical modifications to achieve unprecedented levels of heat transfer efficiency. Moreover, various materials have been tested to check their influence on heat transfer performance.

The central research question is: "What are the effects of different geometries and design modifications on heat transfer properties in heat exchangers?"

The main objective of this study is to analyze the heat transfer process on a heating surface of a heat exchanger under the hot exhaust gas heat transfer as an effect of the natural gas combustion process and investigate its impact on hot water generation. The effect of the heat exchanger geometry in terms of design and enhancement features on the heat transfer process will be analyzed using CFD numerical simulations.

To achieve this aim, a numerical model of the boiler heat exchanger will be taken into account during simulations. The heat transfer process between the hot flue gas flowing inside and water circulating outside tubes respectively for two types of tubes: normal and finned will be studied and compared.

Based on the scientific sources several parameters connected to the analyzed process will be selected. To simulate the heat transfer process in all concerned cases and describe the corresponding species transport and heat radiation the CFD ANSYS Fluent software will be used.

In this research paper, the working fluids used in a low-temperature boiler with 30 kW thermal capacity and around 90% efficiency are analyzed in detail. The focus of the investigation is on the ambient air condition, which serves as an oxidizer for the combustion process occurring inside the furnace. The ambient air, mixed with natural gas GZ 50 in a 20% air excess ratio, will be examined to determine its impact on the combustion process.

There is a set of techniques that could be used to optimize the heat transfer as a process. Extended surfaces (fins) and devices to generate swirl flow (turbulators) are the most familiar elements added to the heat exchanger tube [5].

In the computational analysis conducted, the governing equations for fluid flow and heat transfer were solved to capture the intricate interactions within the water boiler system. The selected turbulence model RNG-k-ε, P-1 Radiation model, and Species transport were integrated into the computational

framework provided by ANSYS Fluent. The following governing equations were solved to represent the physical phenomena under investigation:

Continuity Equation:

The continuity equation (1) describes the conservation of mass within the system and is expressed as follows:

$$\frac{\partial t}{\partial \rho} + \nabla \cdot (\rho \boldsymbol{V}) = 0 \qquad (1)$$

Momentum Equation:

The momentum equation accounts for the conservation of linear momentum and is given by equation (2):

$$\frac{\partial (\rho \boldsymbol{V})}{\partial t} + \nabla \cdot (\rho \boldsymbol{V} \otimes \boldsymbol{V}) = -\nabla P + \nabla \cdot \boldsymbol{\tau} + \rho \boldsymbol{g} \qquad (2)$$

Energy Equation:

The energy equation (3) represents the conservation of energy and includes contributions from conduction, convection, and radiation. It is formulated as:

$$\frac{\partial (\rho h)}{\partial t} + \nabla \cdot (\rho \boldsymbol{V} h) = \nabla \cdot (\alpha \nabla T) + \dot{q} \qquad (3)$$

The mathematical equations underpinning these models, collectively simulating the physical phenomena of interest, were applied uniformly to the entire computational mesh. The finite volume method with a SIMPLE model was employed for this purpose, where each discretized cell within the mesh serves as a representative model element. This approach allows for the comprehensive analysis of the system and the evaluation of critical parameters.

The simulation process was carried out iteratively, with calculations performed sequentially to ensure the convergence of results. This iterative mode was crucial for reaching a stable and accurate solution, ultimately enabling a comprehensive understanding of the heat transfer and fluid flow dynamics within the examined system.

The results of the simulations performed were analyzed to determine the effect of finned tubes and different tube materials on the heat transfer process of the heat exchanger.

2. Materials and Methods

A. Model description

Heat exchanger data and dimensions

The heat exchanger, which was taken under investigation comprises a set of 20 tubes, Fig. 1.

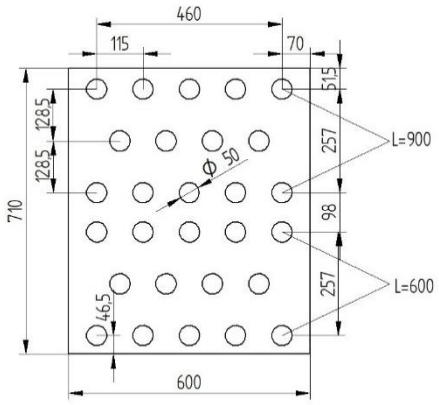

Fig. 1. The view of full heat exchanger plate showing tubes alignment

However, for the analysis across the considered cases only two tubes were selected, Fig. 2.

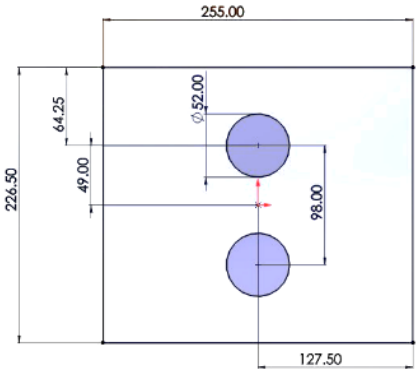

Fig. 2. Selected study region

The tubes used in the heat exchanger consist of two solid materials and two fluids by default in all cases, Fig. 3.

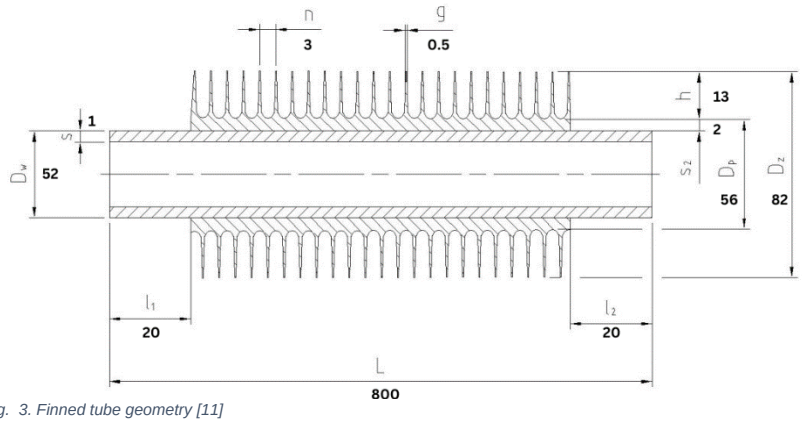

Fig. 3. Finned tube geometry [11]

To determine the performance of the heat exchanger, further equations and procedures were used to calculate data related to the composition of flue gases resulting from fuel combustion and temperature.

The ambient air parameters selected as inputs for this study encompass an atmospheric pressure of 101.325 kPa and an ambient temperature of 20°C. The natural gas under consideration (Natural gas GZ 50) is characterized by an ambient pressure of 2.5 kPa and an ambient temperature of 23°C. These specific environmental conditions serve as the foundational reference points for our investigation into the heat transfer processes and combustion dynamics within the system

Algorithm of calculation

To calculate the mass flow rate of water in the boiler, we utilized the isobaric process and the thermal capacity of the boiler, as described in equation (4) :

$$\dot{Q}_{uh} = \dot{m}_w \cdot c|_{t'_w}^{t''_w} \cdot (t''_w - t'_w) = \rho_{w_{av}} \cdot \dot{V}_w \cdot c|_{t'_w}^{t''_w} \cdot (t''_w - t'_w), \qquad (4)$$

The mass flow rate of water in the boiler was calculated by assuming the isobaric heating process and the thermal capacity of the boiler, as described in equation (1). Taking into consideration the water boiler's thermal capacity of 30 kW, the calculation was then performed.

After calculating the volumetric water mass flow rate, the next step is to determine the chemical energy supplied with the natural gas GZ 50. This can be achieved by using the equation of the direct method efficiency formula from equation (5):

$$\eta_b = \frac{\dot{Q}_{uh}}{\dot{E}_{ch}} \qquad (5)$$

Natural gas GZ 50 composition is as follows [6]:

$[CH_4]$ = 98%,
$[C_2H_6\ ]$ =1%,
[N₂] = 1%.

The calorific value of the fuel can be calculated from the equation (6):

$$Q_i = CH_4 \cdot 354.1 + C_2H_6 \cdot 635.2 \qquad (6)$$

After calculating the calorific value of the fuel using Equation (6) and the chemical energy of the natural gas GZ 50 using Equation (5), the volumetric flow rate of the flue gas can be determined using Equation (7). This equation relates the volumetric flow rate of the flue gas to the mass flow rate of the fuel and the density of the flue gas:

$$\dot{E}_{ch} = \dot{Q}_i \cdot \dot{V}_{fuel} \qquad (7)$$

Furthermore, additional equations and procedures were used to determine data related to the composition of the flue gases resulting from the fuel combustion process. The temperature of the flue gases was also assumed based on market values and resources where the temperature was considered to be 1273.15 K. These assumptions were necessary to complete the analysis and obtain the relevant data for the system.

It is important to note that the calculations presented in this section were made based on assumed data and utilizing information regarding the heat exchanger dimensions and specifications. These parameters were used to determine input values for the system, as presented in Tables 1 and 2 respectively. Furthermore, for a comprehensive understanding of the system, Table 3 has been incorporated to delineate the material properties essential for the analysis.

Table 1. Flue gas composition

Species	[%]
H_2O	17.38
CO_2	6.19
O_2	4.33
N_2	72.08
Total	100.00

Table 2. CFD modeling data

	unit	full heat exchanger	selected domain
area ratio	-	1	0.425
Water mass flow rate	kg/s	0.477	0.203
flue gas velocity	m/s	5.564	0.278
water inlet temperature	K	313.15	
flue gas inlet temperature	K	1273.15	

Table 3. Material properties of fins used in the simulation [7]

Physical property	**Thermal conductivity**	**Density**	**Specific heat C_p**
Unit	[W/ (m K)]	[kg/m^3]	[J/ (kg K)]
Copper	387.60	8978	381.00
Aluminum	202.40	2719	871.00
Steel	16.27	8030	502.48

Numerical model

The study involved preparing tubes using SOLIDWORKS CAD software (Fig. 4) and importing them to ANSYS SpaceClaim and Design Modeler for further preparation to ensure compatibility with the software.

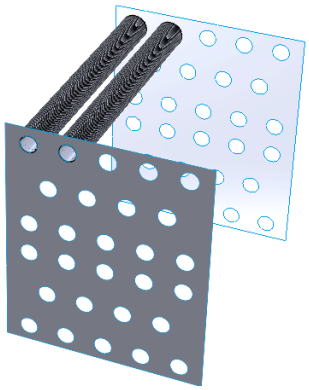

Fig. 4. 3D CAD rendering of the selected study region of finned tube case

The enclosure alternative was created using the Boolean feature, which was the main preparation feature in Design Modeler. The modeling process was divided into two parts: unfinned tube modeling (Fig. 5) and finned tube modeling (Fig. 6).

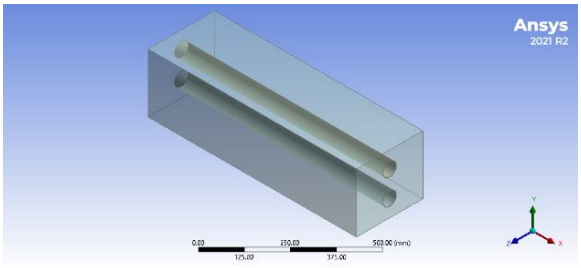

Fig. 5. Unfinned tube's isometric view

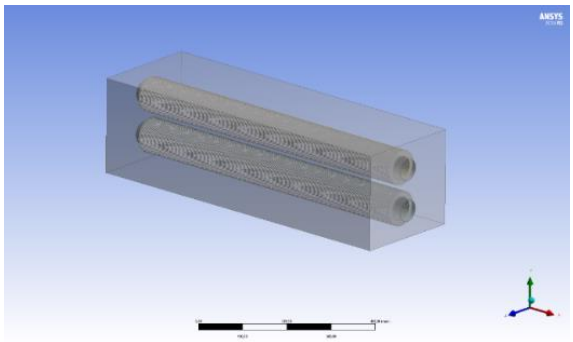

Fig. 6. Finned tube's isometric view

Mesh Independence Study

In exploring mesh independence, various mesh sizes from 250 mm to 4 mm, that correspond to 57 974 and 882 764 elements respectively, were systematically examined. To quantitively define the mesh independency, temperature's percentage deviation ω between the finest and i^{th} mesh has been presented in Eq. (8). As a common practice [8] [9], when $\omega < 1\%$ the results were assumed as a mesh independent The data presented in Fig. 7, depicting temperatures and deviations across different mesh elements, revealed a significant observation: the water temperature stabilized and the deviation ω is lower than 1% around a 5 mm (437 920 elements) mesh size, suggesting mesh independence. This alignment with predefined convergence criteria boosts confidence in the simulation results. The decision to settle on a 5 mm mesh size is a thoughtful choice, considering a balance between accurate results and computational efficiency.

$$\omega = \frac{T_i - T_{finest}}{T_{finest}} \times 100\% \qquad (8)$$

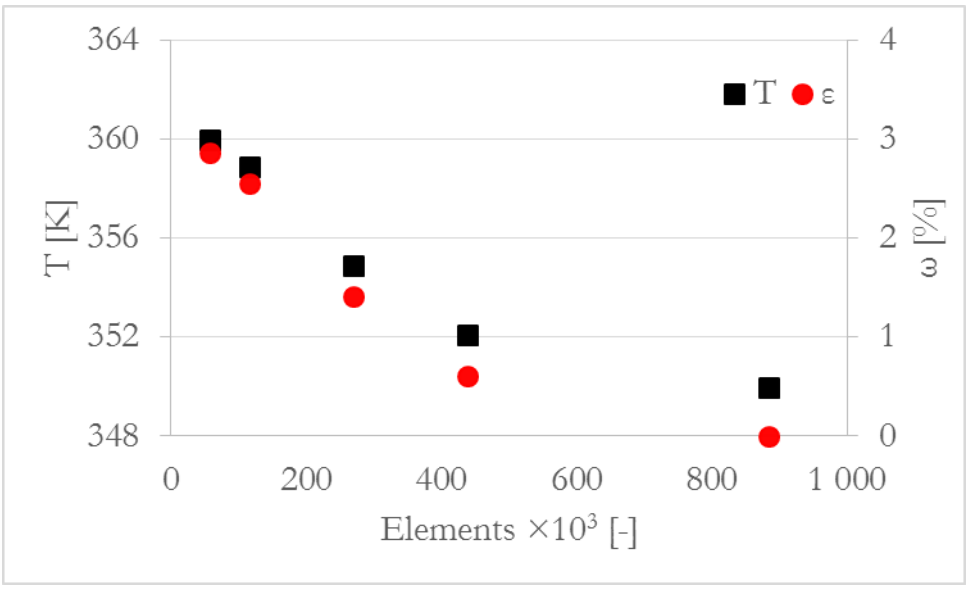

Fig. 7. Mesh Independence Study

Mesh data, representing the mesh element number generated as model discretization with mesh orthogonal quality of 0.9975 and 0.61496 on average for 437 920 and 3 383 495 elements for the unfinned and finned model respectively, which is referring to Ansys theory guide high quality of the mesh [10].

During the simulation, residual values for key parameters, including energy, XYZ velocities, turbulence variables (k and ε), and species concentrations (H_2O, O_2, N_2, CO_2), along with pressure (P1), were closely monitored. These residuals exhibited stable behavior, with values remaining consistent and not showing significant decreases, indicating a convergence level within the range of at least 1e-3. This stable behavior is a positive indicator of convergence for the simulation, implying that the solution reached a satisfactory level of accuracy.

The solid cell condition of the tube and fins was assigned as steel, copper, or aluminum. The fluid mixture used in the flue gas is a species with a calculated volume ratio. Water fluid was defined to be entering the heat exchanger and flowing over and around the flue gas tube so it would gain heat and proceed to the outside. Fig. 8. shows a picture of how the model is set up.

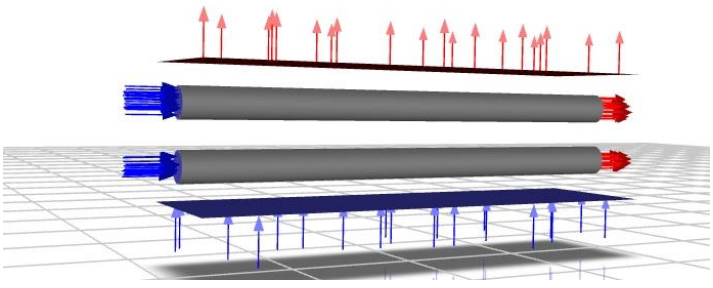

Fig. 8. ANSYS Fluent heat exchanger model scheme

3. Results

A. Numerical Test Interpretation

The outlet temperature of the water is a key parameter to compare and evaluate the performance of the finned and unfinned cases. The outlet temperatures of the flue gases and the outer fluid are also included for completeness but are not considered in the main study.

The temperature difference between the fluids between the inlet zone and the outlet zone is shown in Eq. (5).

$$\Delta T = t_{inlet} - t_{outlet} \text{ [K]} \qquad (5)$$

The material of the tube is the main variable in the study, while the material of the fins is fixed as aluminum for the finned case.

Table 4. Outer fluid and flue gases input temperature

Input fluid parameters		
T_{water_inlet}	[K]	313.15
$T_{fg\_inlet\_1}$	[K]	1273.15
$T_{fg\_inlet\_2}$	[K]	1273.15

B. Numerical Test Results

Unfinned Tubes

The water fluid temperature difference shows the role of the tube material in the heat transfer phenomenon. By the chart which is represented in Fig. 9, it can be noted that copper recorded ΔT= 3.1 K higher than that for Aluminum and Steel with ΔT=2.6 K, and ΔT= 2.5 K respectively.

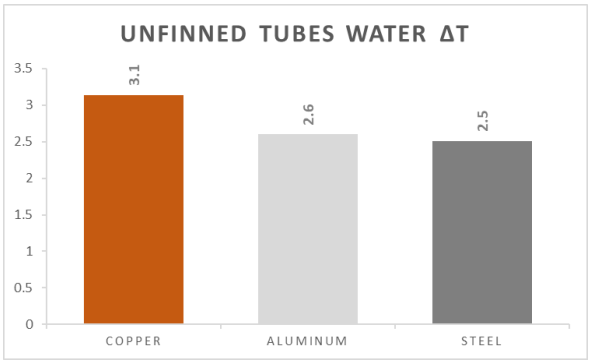

Fig. 9. Unfinned tube model water ΔT temperature by material

Finned Tubes

Water fluid temperature rise (ΔT) shows the role of the tube material on the heat transfer phenomenon, but in this section, aluminum fins were added to the tubes. Referring to the graph of Fig. 10, it can be noted that copper recorded ΔT = 18 K higher than that for Aluminum and Steel with ΔT = 17.2 K, and ΔT = 16.4 K respectively.

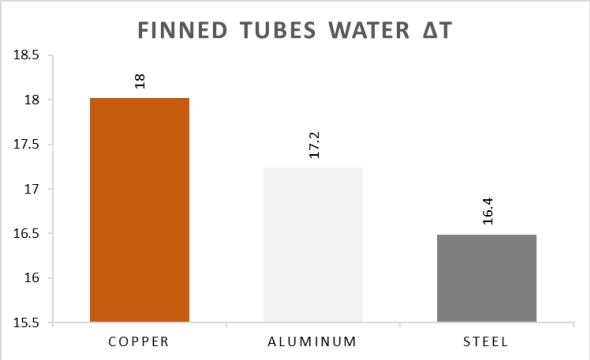

Fig. 10. Finned tube model water ΔT temperature by material

4. Discussion

Numerical result Investigations

The column graph in Fig. 11, shows the comparison data between two models: regular unfinned tubes and tubes equipped with aluminum fins. The first three cases of study involved changing the tube's material (copper, steel, and aluminum). While studying the behavior of the water temperature as an outer fluid circulated the tubes filled with flue gases passing inside, a higher effect of ΔT was observed for the finned tubes in all three materials. The average difference of ΔT between the finned tubes and the unfinned ones was around 15 K.

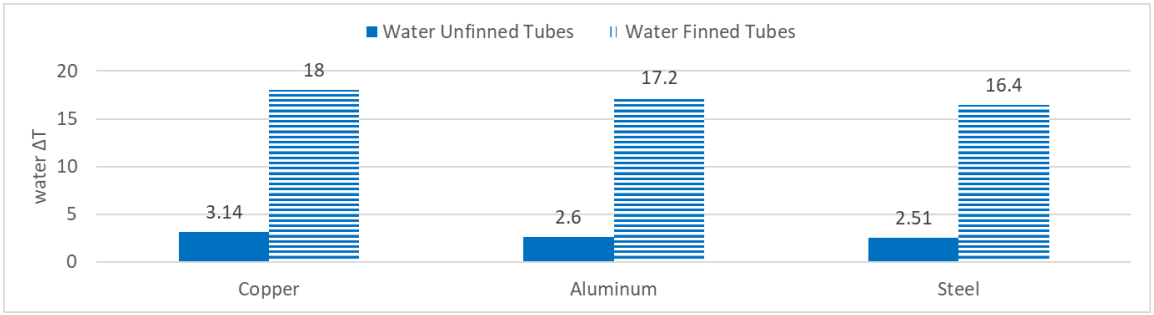

Fig. 11. Finned-Unfinned models water ΔT temperature column graph

Contours Interpretation

This section presents a graphical analysis of two distinct cases of water as the heated fluid, using both unfinned and finned tubes. The tube material selected for both cases is copper, while aluminum is used for the fins in the finned case.

The 3D rendering of the model presented in Fig. 12 depicts the physical phenomenon of heat transfer in the studied system. The cold water at a temperature of 313.15 K enters from the bottom to interact with the first tube, which holds flue gas flowing inside. As a result of this interaction, the water gains heat and proceeds to flow through the second tube, where the temperature profile is higher on that tube wall. The water outlet surface also shows a higher temperature due to the transfer of heat between the water and flue gas passing inside the copper tubes through the mechanisms of heat transfer.

Similarly, Fig. 13 focuses on the addition of fins. Once again, the cold water at a temperature of 313.15 K enters from the bottom and interacts with the first tube, holding flue gas flowing inside, gaining heat.

As a result, the hotter water flows through the second tube, where the temperature profile is again higher on that tube wall. The addition of fins further enhances the heat transfer between the water and the flue gas, resulting in an even higher temperature at the water outlet surface. Fig. 14 shows the static temperature contours of the mid-plane intersecting the whole model exactly in the middle. The next figure which is Fig. 15 represents the wall temperature of the same plane, here the profile is different due to the presence of fins (Aluminum). It is important to note that while the 3D renders depict both the water and flue gas, the study interest focused only on the outer fluid temperature.

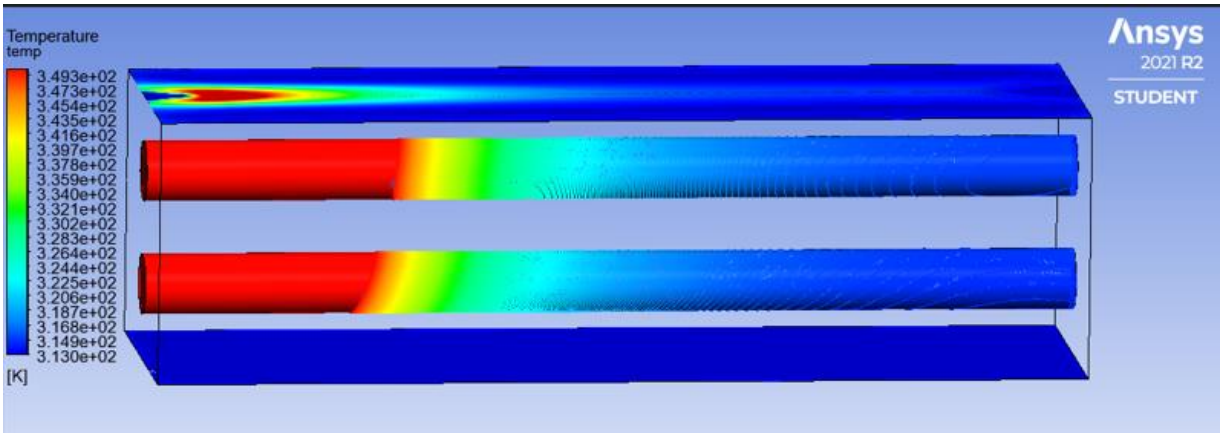

Fig. 12. UnFinned tubes with inlet and outlet 3D ANSYS post processor render

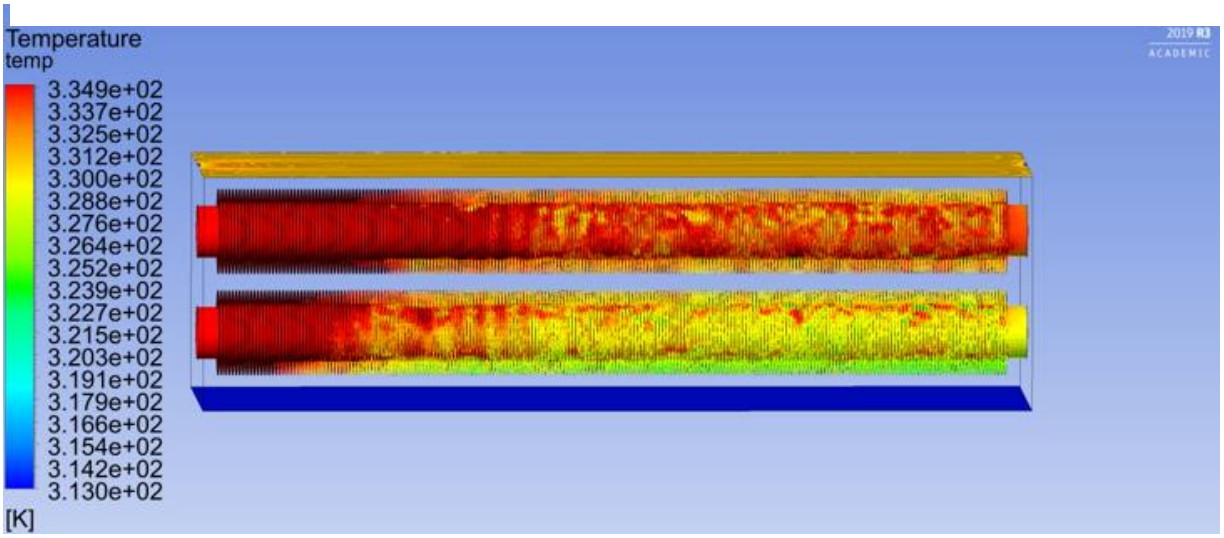

Fig. 14. Finned tubes with inlet and outlet 3D ANSYS post processor render

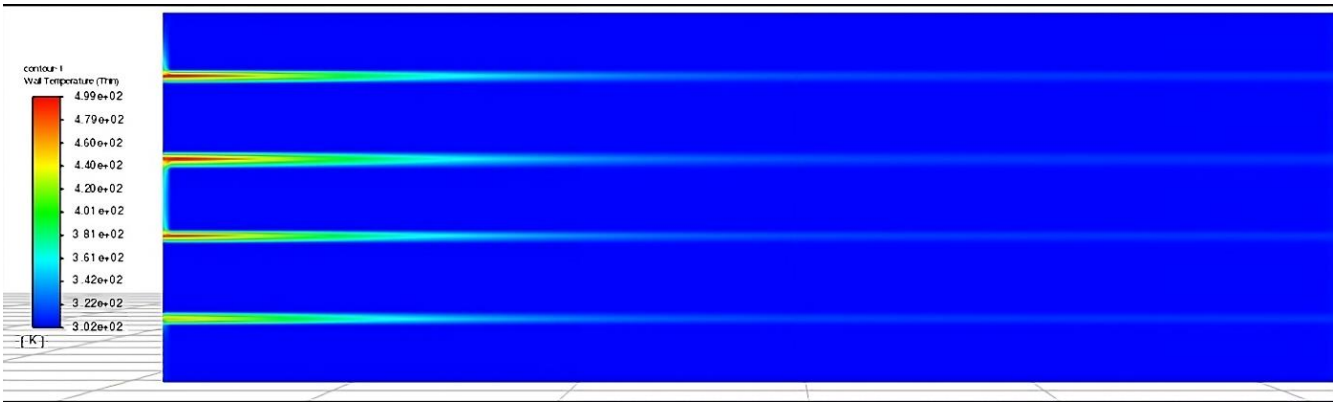

Fig. 13. UnFinned water copper wall temperature mid-plane contour

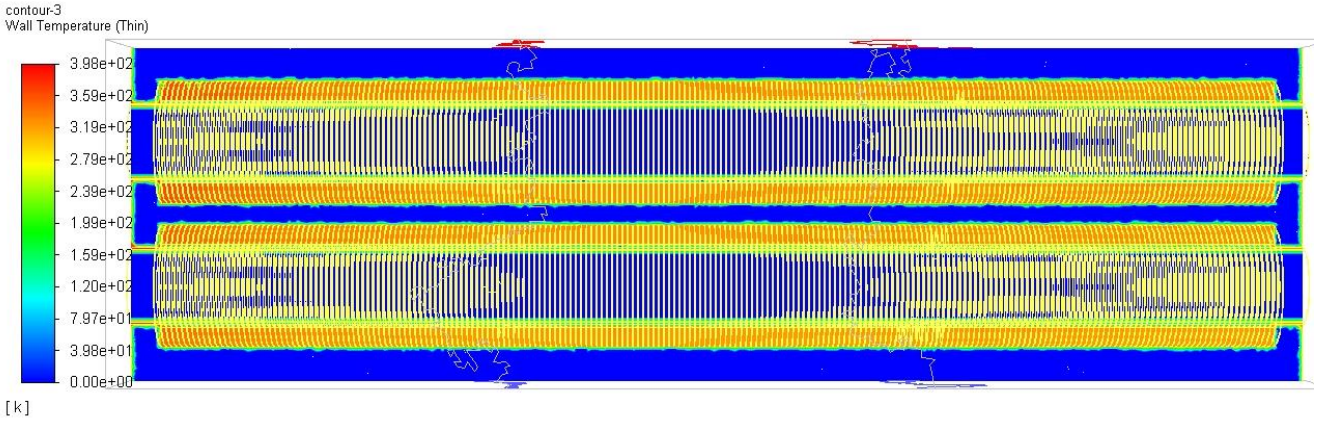

Fig. 15. Finned water copper wall temperature mid-plane contour

5. Conclusion

After performing a set of simulations and interpreting the output data, it can be concluded that copper has the highest capability to heat transfer, followed by aluminum and steel for the tubes carrying flue gas. Transverse aluminum fins were added and recorded a massive change in the heat transfer process.

Heat transfer occurs inside the heat exchanger, and takes place through three mechanisms: radiation, conduction, and convection. The first mechanisms are radiation and convection between the fluid passing through the tubes and the tube's inner wall. The second is the conduction through the tube's solid wall, which is directly proportional to the material's thermal conductivity and contact area.

In the conduction operation, the wall of the tube and the tube's fins will be thermally coupled. The fins will interact with the outer fluid, supporting the process of transferring heat through conduction with the tube carrying fluid inside and through convection with the outer fluid.

From the output data and the contours, it can be concluded that materials with high thermal conductivity, coupled with fins, will enhance the heat transfer process. However, other factors such as design requirements, ease of manufacturing, market availability, and operational cost should also be taken into consideration.

The findings of this research will provide valuable insights into the design and optimization of heat exchangers for various industrial applications.

CRediT author statement:

Abdullah El Sabea: Conceptualization, Data Curation; Formal Analysis; Investigation; Software; Visualization; Writing – original draft

Jacek Baranski: Investigation; Methodology; Validation; Writing – review & editing; Conceptualization, Resources; Project Administration; Supervision

Paweł Dąbrowski: Formal Analysis, Visualization, Writing – review & editing.

Conflicts of Interest: The authors declare no conflicts of interest.

References

[1] J. Smith, "Water Heaters Global Market Report 2022," ReportLinker, New York, 2022.

[2] U. U. Rehman, "Heat Transfer Optimization of Shell-and-Tube," Chalmers University of Technology, Goteborg, Sweden, 2011.

[3] M. Rajeshkumar, L. Kamaraj, S. Govindan and M. Thangaraj, "Heat transfer study on finned tube heat exchanger using CFD," *International Journal of Ambient Energy ,* pp. 239-243, 2018.

[4] S. Kaushik, S. Sharma and V. S. Chamyal, "Numerical Investigation of Boiler Tubes for Performance of Heat Transfer Enhancement with Varying Shapes of Corrugated Tube," *International Journal of Engineering Research and Applications,* pp. 46-54, 2017.

[5] S. Tabatabaeikia, H. A. Mohammed, N. N. Nik Ghazali and B. Shahiraze, "Heat Transfer Enhancement by Using Different Types of Inserts," *Advances in Mechanical Engineering,* 2014.

[6] M. Wilk, "Ozone impact on NO emission in natural gas combustion: a numerical and experimental study," *AGH University of Science & Technology,* p. 12, 2016.

[7] T. N. I. o. S. a. T. (NIST), "Property Tables and Charts (SI UNITS)," cecs.wright.edu, Gaithersburg, 2010.

[8] P. Dąbrowski, "Thermohydraulic maldistribution reduction in mini heat exchangers," *Applied Thermal Engineering,* vol. 173, no. 115271, 2020.

[9] R. Kumar, G. Singh and D. Mikielewicz, "A new approach for the mitigating of flow maldistribution in parallel microchannel heat sink," *Journal of Heat Transfer,* vol. 140, no. 027401, 2018.

[10] Ansys, "Excellence in Engineering Simulation," *Advantage,* vol. 8, no. 1, p. 6, 2014.

[11] CEMAL, "High Extension Bimetal Pipe RBW," CEMAL, 01 06 2016. [Online]. Available: https://cemal.com.pl/oferta/rura-bimetalowa-wysokozebrowana-rbw/.